

STRUCTURAL STUDY ON 1-PHENYL- AND 1-(2-NAPHTHYL)-8-TROPYLIONAPHTHALENE HEXAFLUOROANTIMONATES

RYOTARO TSUJI, KOICHI KOMATSU* AND KEN'ICHI TAKEUCHI

Department of Hydrocarbon Chemistry, Faculty of Engineering, Kyoto University, Sakyo-ku, Kyoto 606-01, Japan

MOTOO SHIRO

Rigaku Corporation, 3-9-12 Matsubara-cho, Akishima, Tokyo 196, Japan

AND

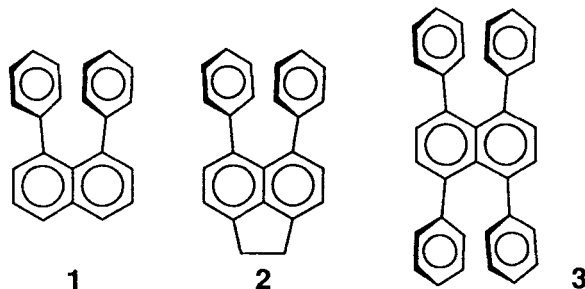
SHMUEL COHEN AND MORDECAI RABINOVITZ*

Department of Organic Chemistry, Hebrew University of Jerusalem, Jerusalem 91904, Israel

The molecular structures of 1-phenyl- (5) and 1-(2-naphthyl)-8-tropyliumnaphthalene (6) hexafluoroantimonates were determined by x-ray crystallography and compared with those of 1,8-diphenylnaphthalene and related compounds. In these compounds, the two aromatic substituents face each other in a nearly parallel conformation with a splayed-out arrangement. In the cations 5 and 6, the distance between the facing rings is appreciably shorter than that of other 1,8-diarylnaphthalenes, suggesting the presence of some attractive force. This attraction is ascribed to an intramolecular charge-transfer interaction, and seems to bring about a slight inward bending of the 2-naphthyl substituent in the cation 6. AM1 calculations were carried out for these cations and the results are discussed in comparison with the results of x-ray crystallography.

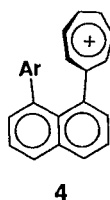
INTRODUCTION

The nature of π - π interactions between stacked aromatic rings is attracting considerable interest, and both theoretical and experimental studies are being carried out for its elucidation.¹ Such interactions can be roughly divided into electronic (Coulombic) and van der Waals terms. As representative model compounds having two phenyl rings which are fixed intramolecularly in close proximity without too much molecular strain, a series of *peri*-substituted naphthalenes, 1,8-diphenylnaphthalene (1),² 1,8-diphenylacenaphthene (2)³ and 1,4,5,8-tetraphenylnaphthalene (3),⁴ have been synthesized and their structures determined by x-ray crystallography. In these compounds the phenyl rings are forced to take a stacked arrangement with an essentially face-to-face conformation. However, both the Coulombic and van der Waals interactions operate in a repulsive way so that the two benzene rings are splayed apart and the junction of the naphthalene moiety is slightly distorted out of plane.



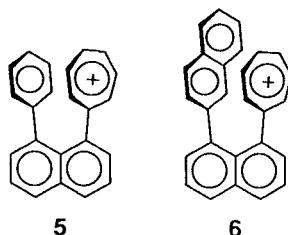
On the other hand, we have previously reported the syntheses and properties of a series of 1-aryl-8-tropyliumnaphthalenes (4).⁵ In these cations, the intramolecular charge-transfer interaction between a neutral aromatic ring (donor) and a cationic tropylium ring (acceptor) was found to contribute greatly to the thermodynamic stabilization of the tropylium ion, whereas Cozzi *et al.*^{1c} recently reported that a 'through-space Coulombic interaction' rather than a charge-transfer interaction exists predominantly between the two differ-

* Authors for correspondence.



ently substituted benzene rings in 1,8-diarylnaphthalenes. The charge-transfer interaction in the tropylium ion derivative **4** is expected to exert an attractive force for the two facing aromatic rings. Therefore, the effects of such interaction on the molecular geometry of these rings are of particular interest.

In this paper, we report the results of x-ray structure determination and theoretical calculations on 1-phenyl- (5) and 1-(2-naphthyl)-8-tropyliumnaphthalenes (**6**) as typical examples of the intramolecular charge-transfer cation **4**. The x-ray crystallography of **1** was also conducted since the details of the previously determined data^{2b} have not been published or stored in the Cambridge Data Base.⁶



EXPERIMENTAL

1,8-Diphenylnaphthalene (**1**) was prepared by cross-coupling of phenylmagnesium iodide with 1,8-diiodonaphthalene catalysed by nickel(II) acetylacetonate.^{2c} 1-Phenyl-8-tropyliumnaphthalene hexafluoroantimonate (**5**·SbF₆⁻)^{5a} and 1-(2-naphthyl)-8-tropyliumnaphthalene hexafluoroantimonate (**6**·SbF₆⁻)^{5b} were prepared as reported previously. A single crystal of **1** was grown from ligroin, whereas those of **5**·SbF₆⁻ and **6**·SbF₆⁻ were grown from dichloromethane-tetrachloromethane and from dichloromethane, respectively. Theoretical calculations were performed on FACOM M-780/30 and FACOM VP-400E computers at the Kyoto University Data Processing Center.

Crystallography. 1-Phenyl- (**5**·SbF₆⁻) and 1-(2-naphthyl)-8-tropyliumnaphthalene hexafluoroantimonates (**6**·SbF₆⁻). Diffraction data were measured on a Philips PW1100/20 four-circle computer-controlled diffractometer. Mo K α ($\lambda = 0.71069 \text{ \AA}$) radiation with a graphite crystal monochromator in the incident beam was used. The unit cell dimensions were obtained by a least-squares fit of 24 centred reflections in the range $10^\circ \leq \theta \leq 15^\circ$ for **5**·SbF₆⁻ and $12^\circ \leq \theta \leq 15^\circ$ for **6**·SbF₆⁻. Intensity data were collected using the $\omega - 2\theta$ technique to a maximum 2θ of 50° . The scan width, $\Delta\omega$, for each reflection was $(1.00 + 0.35 \tan \theta)^\circ$ with a scan speed of $3.0^\circ \text{ min}^{-1}$. Background measurements were made for a total of 20 s at both limits of each scan. Three standard reflections were monitored every 60 min. No systematic variations in intensities were found.

Table 1. Crystal data and data collection parameters

Parameter	5·SbF ₆ ⁻	6·SbF ₆ ⁻	1
Empirical formula	C ₂₃ H ₁₇ F ₆ Sb	C ₂₇ H ₁₉ F ₆ Sb	C ₂₂ H ₁₆
Molecular weight	529.13	579.19	280.37
Appearance	Orange, needle	Red-orange, needle	Colourless, prismatic
Space group	Monoclinic, <i>P2</i> ₁ / <i>c</i>	Triclinic, <i>P</i> 1	Monoclinic, <i>P2</i> ₁ / <i>n</i>
<i>a</i> (Å)	6.732(2)	11.456(3)	8.585(2)
<i>b</i> (Å)	29.987(5)	15.950(4)	20.025(2)
<i>c</i> (Å)	10.452(2)	6.672(2)	9.649(1)
α (°)	90	95.33(2)	90
β (°)	103.82(4)	99.41(3)	115.849(10)
γ (°)	90	72.68(2)	90
<i>V</i> (Å ³)	2050.4(8)	1149.9(8)	1492.9(4)
<i>Z</i>	4	2	3
<i>d</i> _{calc.} (g cm ⁻³)	1.71	1.68	1.15
μ (cm ⁻¹)	14.10	12.68	4.6
Temperature (°C)	Ambient	Ambient	23 ± 1
No. of unique reflections	3691	4039	2307
No. of observed ^a reflections	2431	3178	1407
<i>R</i>	0.084	0.051	0.039
<i>R</i> _w	0.111	0.068	0.051

^a $I \geq 3\sigma(I)$.

Intensities were corrected for Lorentz and polarization effects. All non-hydrogen atoms were found by using the results of the SHELXS-86 direct method analysis.⁷ The crystallographic computing for $5 \cdot \text{SbF}_6^-$ and $6 \cdot \text{SbF}_6^-$ was done on a VAX computer at the Hebrew University of Jerusalem, using TEXSAN⁸ analysis software. After several cycles of refinements the positions of the hydrogen atoms were calculated and added to the refinement process. Refinement proceeded to convergence by minimizing the function $\Sigma w(|F_o| - |F_c|)^2$. A final difference Fourier synthesis map showed several peaks less than 2 and $1 \cdot 0 \text{ e } \text{Å}^{-3}$ for $5 \cdot \text{SbF}_6^-$ and $6 \cdot \text{SbF}_6^-$, respectively, scattered about the unit cell without a significant feature.

Crystal data and data collection parameters are listed in Table 1.

1,8-Diphenylnaphthalene (1). A crystal of **1** having the approximate dimensions $0 \cdot 40 \times 0 \cdot 20 \times 0 \cdot 10 \text{ mm}$ was mounted on a glass fibre. All measurements were made on a Rigaku AFC5R diffractometer with graphite monochromated $\text{Cu K}\alpha$ ($\lambda = 1 \cdot 54178 \text{ Å}$) radiation and a 12 kW rotating anode generator. Cell constants and an orientation matrix for data collection were obtained from a least-squares refinement using the setting angles of 25 carefully centred reflections in the range $54 \cdot 19^\circ < 2\theta < 56 \cdot 97^\circ$. The data were collected using the $\omega - 2\theta$ scan technique to a maximum 2θ value of $120 \cdot 1^\circ$. Omega scans of several intense reflections, made prior to data collection, had an average width at half-height of $0 \cdot 19^\circ$ with a take-off angle of $6 \cdot 0^\circ$. Scans of $(1 \cdot 52 + 0 \cdot 30 \tan \theta)^\circ$ were made at a speed of $16 \cdot 0^\circ \text{ min}^{-1}$ (in omega). The weak reflections [$I < 10 \cdot 0\sigma(I)$] were rescanned (maximum of one rescan) and the counts were accumulated to ensure good counting statistics. Stationary background counts were recorded on each side of the reflection. The ratio of peak counting time to background counting time was 2:1. The diameter of the incident beam collimator was 1.0 mm and the crystal to detector distance was 258 mm. The intensities of three representative reflection were measured after every 150 reflections. No decay correction was applied. An empirical absorption correction using the program DIFABS⁹ was applied, which resulted in transmission factors ranging from 0.87 to 1.13. The data were corrected for Lorentz and polarization effects. A correction for secondary extinction was applied (coefficient = $1 \cdot 39217 \times 10^{-5}$).

The structure was solved by the direct method⁷ and expanded using Fourier techniques.¹⁰ The non-hydrogen atoms were refined anisotropically. Hydrogen atoms were included but not refined. The final cycle of full-matrix least-squares refinement was converged with unweighted and weighted agreement factors. The standard deviation of an observation of unit weight was 1.23. The weighting scheme was based on counting statistics and included a factor ($p = 0 \cdot 060$) to

downweight the intense reflections. Plots of $\Sigma w(|F_o| - |F_c|)^2$ versus $|F_o|$, reflection order in data collection, $\sin \theta/\lambda$ and various classes of indices showed no unusual trends. The maximum and minimum peaks on the final difference Fourier map corresponded to $0 \cdot 13$ and $-0 \cdot 12 \text{ e } \text{Å}^{-3}$, respectively.

Neutral atom scattering factors were taken from Cromer and Waber.¹¹ Anomalous dispersion effects were included in Fcalc;¹² the values for $\Delta f'$ and $\Delta f''$ were those of Creagh and McAuley.¹³ The values for the mass attenuation coefficients are those of Creagh and Hubble.¹⁴ All calculations were performed using the TEXSAN⁸ crystallographic software package.

Crystal data and data collection parameters are listed in Table 1.

RESULTS AND DISCUSSION

The determined molecular structures of the cation **5**, the cation **6** and diphenylnaphthalene (**1**) are shown in Figures 1, 2 and 3, respectively, and the stereoscopic views of the unit cells of $5 \cdot \text{SbF}_6^-$, $6 \cdot \text{SbF}_6^-$ and **1** are shown in Figures 4, 5 and 6, respectively. The bond lengths and angles for **5**, **6** and **1** are given in Tables 2, 3 and 4, respectively.

The head-on views (normal to the substituents) and the side views (parallel to the substituents) for **5** and **6**

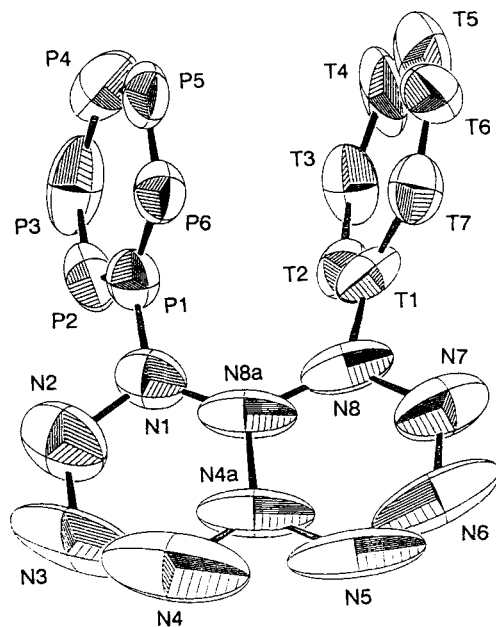


Figure 1. X-ray crystal structure of 1-phenyl-8-tropyliumaphthalene (**5**) with the numbering of the atoms. Hydrogen atoms are omitted for clarity

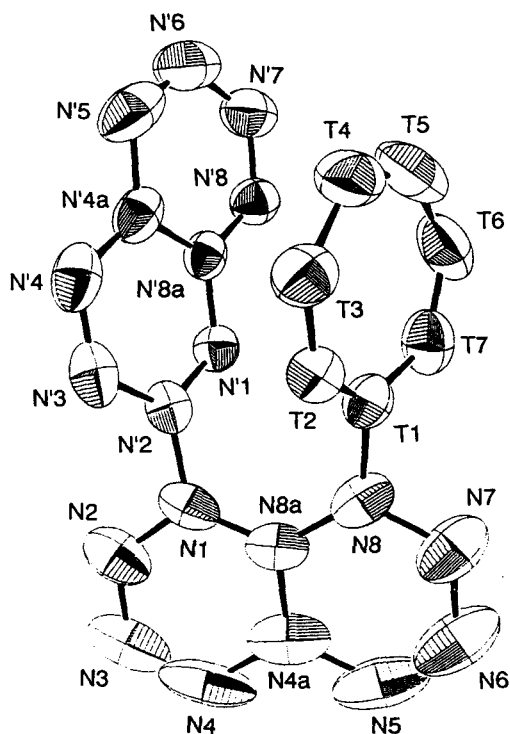


Figure 2. X-ray crystal structure of 1-(2-naphthyl)-8-tropylium naphthalene (**6**) with the numbering of the atoms. Hydrogen atoms are omitted for clarity

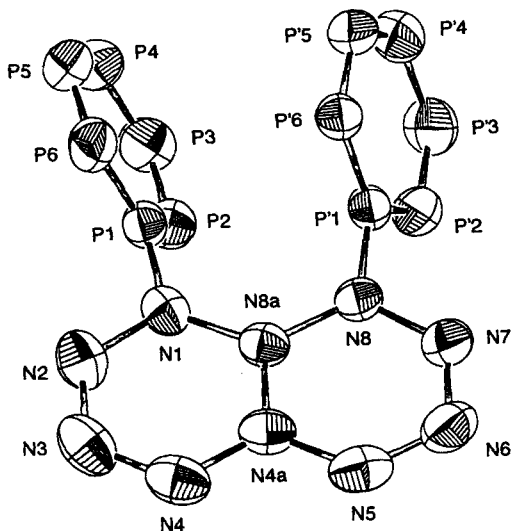


Figure 3. X-ray crystal structure of 1,8-diphenylnaphthalene (**1**) with the numbering of the atoms. Hydrogen atoms are omitted for clarity

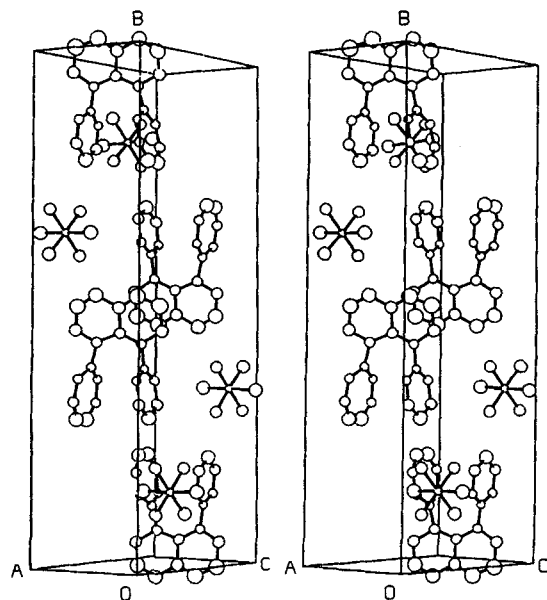


Figure 4. Stereoscopic view of the unit cell of $5 \cdot \text{SbF}_6^-$. Hydrogen atoms are omitted for clarity

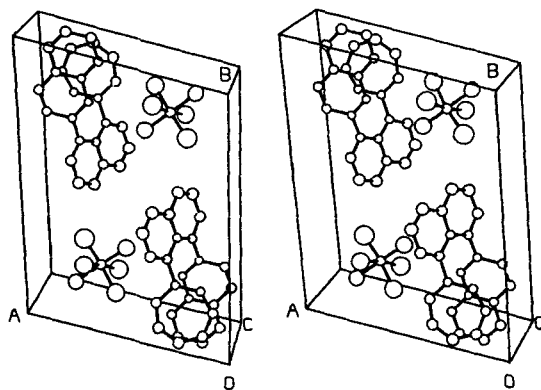


Figure 5. Stereoscopic view of the unit cell of $6 \cdot \text{SbF}_6^-$. Hydrogen atoms are omitted for clarity

are shown in Figure 7 together with those of the 1,8-diphenyl derivative **1** for comparison. It is clearly seen that in both of the cations the two aromatic substituents face each other in a nearly parallel arrangement. A closer examination of the structure of **6** in Figure 7 shows that the 2-naphthyl substituent is slightly folded inward to the face of the tropylium ring. Hence the 2-naphthyl group is not planar: the angle between the C(N-1)—C(N'-2) bond and the best plane formed

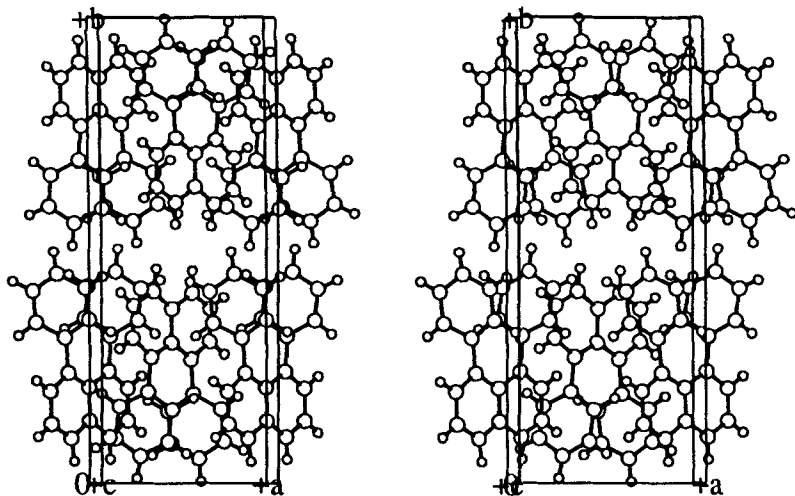


Figure 6. The stereoscopic view of the unit cell of 1

Table 2. Bond lengths and bond angles for $5 \cdot \text{SbF}_6^-$ with esd values in parentheses

Bond	Length (Å)	Bond	Angle (°)
C(N1)—C(N2)	1.40(3)	C(N1)—C(N8a)—C(N8)	129(2)
C(N1)—C(N8a)	1.39(3)	C(N1)—C(N8a)—C(N4a)	120(3)
C(N2)—C(N3)	1.50(6)	C(N8)—C(N8a)—C(N4a)	111(3)
C(N3)—C(N4)	1.37(8)	C(N2)—C(N1)—C(N8a)	117(2)
C(N4)—C(N4a)	1.25(6)	C(N1)—C(N2)—C(N3)	120(3)
C(N4a)—C(N5)	1.48(6)	C(N2)—C(N3)—C(N4)	117(4)
C(N4a)—C(N8a)	1.50(2)	C(N3)—C(N4)—C(N4a)	125(6)
C(N5)—C(N6)	1.24(6)	C(N4)—C(N4a)—C(N5)	118(3)
C(N6)—C(N7)	1.39(4)	C(N4)—C(N4a)—C(N8a)	120(5)
C(N7)—C(N8)	1.40(3)	C(N5)—C(N4a)—C(N8a)	122(4)
C(N8)—C(N8a)	1.41(3)	C(N4a)—C(N5)—C(N6)	118(4)
C(N1)—C(P1)	1.47(3)	C(N5)—C(N6)—C(N7)	126(4)
C(N8)—C(T1)	1.48(3)	C(N6)—C(N7)—C(N8)	117(3)
C(P1)—C(P2)	1.38(2)	C(N7)—C(N8)—C(N8a)	125(2)
C(P1)—C(P6)	1.38(2)	C(N2)—C(N1)—C(P1)	118(2)
C(P2)—C(P3)	1.40(3)	C(N8a)—C(N1)—C(P1)	125(2)
C(P3)—C(P4)	1.53(4)	C(N7)—C(N8)—C(T1)	110(3)
C(P4)—C(P5)	1.49(4)	C(N8a)—C(N8)—C(T1)	124(2)
C(P5)—C(P6)	1.39(3)	C(N1)—C(P1)—C(P2)	118(2)
C(T1)—C(T2)	1.41(2)	C(N1)—C(P1)—C(P6)	119(2)
C(T1)—C(T7)	1.42(2)	C(P2)—C(P1)—C(P6)	123(2)
C(T2)—C(T3)	1.39(3)	C(P1)—C(P2)—C(P3)	122(2)
C(T3)—C(T4)	1.30(4)	C(P2)—C(P3)—C(P4)	117(2)
C(T4)—C(T5)	1.14(5)	C(P3)—C(P4)—C(P5)	117(2)
C(T5)—C(T6)	1.34(4)	C(P4)—C(P5)—C(P6)	119(2)
C(T6)—C(T7)	1.35(3)	C(P1)—C(P6)—C(P5)	121(2)
Sb—F(1)	1.82(1)	C(N8)—C(T1)—C(T2)	122(2)
Sb—F(2)	1.85(1)	C(N8)—C(T1)—C(T7)	119(2)
Sb—F(3)	1.88(1)	C(T2)—C(T1)—C(T7)	119(2)
Sb—F(4)	1.82(1)	C(T1)—C(T2)—C(T3)	128(2)
Sb—F(5)	1.857(9)	C(T2)—C(T3)—C(T4)	132(2)
Sb—F(6)	1.87(1)	C(T3)—C(T4)—C(T5)	131(5)
		C(T4)—C(T5)—C(T6)	129(4)
		C(T5)—C(T6)—C(T7)	130(3)
		C(T1)—C(T7)—C(T6)	130(2)

Table 3. Bond lengths and bond angles for $6 \cdot \text{SbF}_6^-$ with esd values in parentheses

Bond	Length (Å)	Bond	Angle (°)
C(N1)—C(N2)	1.377(9)	C(N1)—C(N8a)—C(N8)	125.7(5)
C(N1)—C(N8a)	1.419(9)	C(N1)—C(N8a)—C(N4a)	118.1(6)
C(N2)—C(N3)	1.41(1)	C(N8)—C(N8a)—C(N4a)	116.1(6)
C(N3)—C(N4)	1.34(1)	C(N2)—C(N1)—C(N8a)	120.4(6)
C(N4)—C(N4a)	1.44(1)	C(N1)—C(N2)—C(N3)	121.3(9)
C(N4a)—C(N5)	1.43(1)	C(N2)—C(N3)—C(N4)	119.7(8)
C(N4a)—C(N8a)	1.432(8)	C(N3)—C(N4)—C(N4a)	121.7(8)
C(N5)—C(N6)	1.31(1)	C(N4)—C(N4a)—C(N5)	121.5(8)
C(N6)—C(N7)	1.38(1)	C(N4)—C(N4a)—C(N8a)	118.7(8)
C(N7)—C(N8)	1.383(9)	C(N5)—C(N4a)—C(N8a)	119.8(8)
C(N8)—C(N8a)	1.446(9)	C(N4a)—C(N5)—C(N6)	121.4(8)
C(N1)—C(N'2)	1.484(8)	C(N5)—C(N6)—C(N7)	120.9(9)
C(N8)—C(T1)	1.486(8)	C(N6)—C(N7)—C(N8)	121.8(8)
C(N'1)—C(N'2)	1.362(7)	C(N7)—C(N8)—C(N8a)	119.8(6)
C(N'1)—C(N'8a)	1.412(7)	C(N2)—C(N1)—C(N'2)	116.1(6)
C(N'2)—C(N'3)	1.424(8)	C(N8a)—C(N1)—C(N'2)	123.4(5)
C(N'3)—C(N'4)	1.344(9)	C(N7)—C(N8)—C(T1)	114.9(6)
C(N'4)—C(N'4a)	1.422(9)	C(N8a)—C(N8)—C(T1)	125.1(5)
C(N'4a)—C(N'5)	1.423(9)	C(N1)—C(N'2)—C(N'1)	122.1(5)
C(N'4a)—C(N'8a)	1.429(7)	C(N1)—C(N'2)—C(N'3)	119.2(5)
C(N'5)—C(N'6)	1.31(1)	C(N'1)—C(N'2)—C(N'3)	118.7(5)
C(N'6)—C(N'7)	1.41(1)	C(N'2)—C(N'1)—C(N'8a)	122.5(5)
C(N'7)—C(N'8)	1.368(9)	C(N'2)—C(N'3)—C(N'4)	121.0(6)
C(N'8)—C(N'8a)	1.400(8)	C(N'3)—C(N'4)—C(N'4a)	121.1(5)
C(T1)—C(T2)	1.397(8)	C(N'4a)—C(N'5)—C(N'6)	122.1(6)
C(T1)—C(T7)	1.400(8)	C(N'5)—C(N'6)—C(N'7)	121.7(6)
C(T2)—C(T3)	1.363(8)	C(N'6)—C(N'7)—C(N'8)	118.5(7)
C(T3)—C(T4)	1.42(1)	C(N'7)—C(N'8)—C(N'8a)	121.5(6)
C(T4)—C(T5)	1.34(1)	C(N'1)—C(N'8a)—C(N'8)	123.0(5)
C(T5)—C(T6)	1.37(1)	C(N'1)—C(N'8a)—C(N'4a)	117.8(5)
C(T6)—C(T7)	1.39(1)	C(N'8)—C(N'8a)—C(N'4a)	119.1(5)
Sb—F(1)	1.820(5)	C(N'4)—C(N'4a)—C(N'5)	124.2(6)
Sb—F(2)	1.829(6)	C(N'4)—C(N'4a)—C(N'8a)	118.7(5)
Sb—F(3)	1.862(7)	C(N'5)—C(N'4a)—C(N'8a)	117.0(6)
Sb—F(4)	1.865(8)	C(N8)—C(T1)—C(T2)	118.9(5)
Sb—F(5)	1.731(6)	C(N8)—C(T1)—C(T7)	117.1(5)
Sb—F(6)	1.753(6)	C(T2)—C(T1)—C(T7)	123.7(6)
		C(T1)—C(T2)—C(T3)	131.7(6)
		C(T2)—C(T3)—C(T4)	128.1(6)
		C(T3)—C(T4)—C(T5)	128.3(7)
		C(T4)—C(T5)—C(T6)	128.1(7)
		C(T5)—C(T6)—C(T7)	130.4(7)
		C(T1)—C(T7)—C(T6)	129.3(7)

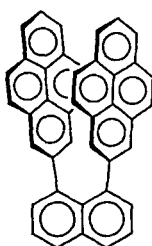
by C(N'-1)—C(N'-3)—C(N'-4)—C(N'-8a) is about 7° , and the dihedral angle between the above-mentioned plane and the best plane formed by C(N'-4a)—C(N'-5)—C(N'-6)—C(N'-7)—C(N'8) is about 4° . As a result of such a deformation, the dihedral angle between the tropylium plane and the A-ring of the naphthyl substituent is 13° and that for the B-ring is 9° .

The structural characteristics of the cations **5** and **6** are summarized in Table 5 together with those of the related compounds **1**, **2**, **3** and 1,8-di(2-pyrenyl)-

naphthalene (**7**).¹⁵ Although a rigorous discussion about the geometry of the cation **5** has to be restricted owing to the large *R* value (see Table 1) originating from the low quality of the crystal in spite of carefully repeated recrystallizations, a qualitative comparison could be safely made based on general tendencies of the structural characteristics. Compared with 1,8-diphenylnaphthalene (**1**), the distances between the two facing aromatic rings are generally shorter in the cations **5** and **6**, suggesting the presence of an attractive interaction. In contrast, the longer distances between

Table 4. Bond lengths and bond angles for **1** with esd values in parentheses

Bond	Length (Å)	Bond	Angle (°)
C(N1)—C(N2)	1·378(3)	C(N1)—C(N8a)—C(N8)	126·2(2)
C(N1)—C(N8a)	1·441(3)	C(N1)—C(N8a)—C(N4a)	116·9(2)
C(N2)—C(N3)	1·396(3)	C(N8)—C(N8a)—C(N4a)	116·9(2)
C(N3)—C(N4)	1·349(3)	C(N2)—C(N1)—C(N8a)	119·5(2)
C(N4)—C(N4a)	1·409(3)	C(N1)—C(N2)—C(N3)	122·6(2)
C(N4a)—C(N5)	1·408(3)	C(N2)—C(N3)—C(N4)	119·3(2)
C(N4a)—C(N8a)	1·439(3)	C(N3)—C(N4)—C(N4a)	121·6(2)
C(N5)—C(N6)	1·353(3)	C(N4)—C(N4a)—C(N5)	119·9(2)
C(N6)—C(N7)	1·398(3)	C(N4)—C(N4a)—C(N8a)	120·2(2)
C(N7)—C(N8)	1·371(3)	C(N5)—C(N4a)—C(N8a)	120·0(2)
C(N8)—C(N8a)	1·437(3)	C(N4a)—C(N5)—C(N6)	121·7(2)
C(N1)—C(P1)	1·498(3)	C(N5)—C(N6)—C(N7)	119·0(2)
C(N8)—C(P'1)	1·494(3)	C(N6)—C(N7)—C(N8)	122·6(2)
C(P1)—C(P2)	1·391(3)	C(N7)—C(N8)—C(N8a)	119·8(2)
C(P1)—C(P6)	1·385(3)	C(N2)—C(N1)—C(P1)	114·7(2)
C(P2)—C(P3)	1·384(3)	C(N8a)—C(N1)—C(P1)	125·8(2)
C(P3)—C(P4)	1·378(3)	C(N7)—C(N8)—C(P'1)	115·8(2)
C(P4)—C(P5)	1·370(3)	C(N8a)—C(N8)—C(P'1)	124·4(2)
C(P5)—C(P6)	1·383(3)	C(N1)—C(P1)—C(P2)	121·8(2)
C(P'1)—C(P'2)	1·394(3)	C(N1)—C(P1)—C(P6)	119·6(2)
C(P'1)—C(P'6)	1·390(3)	C(P2)—C(P1)—C(P6)	118·4(2)
C(P'2)—C(P'3)	1·381(3)	C(P1)—C(P2)—C(P3)	120·4(2)
C(P'3)—C(P'4)	1·373(3)	C(P2)—C(P3)—C(P4)	120·3(2)
C(P'4)—C(P'5)	1·371(3)	C(P3)—C(P4)—C(P5)	119·8(2)
C(P'5)—C(P'6)	1·379(3)	C(P4)—C(P5)—C(P6)	120·2(2)
		C(P1)—C(P6)—C(P5)	120·8(2)
		C(N8)—C(P'1)—C(P'2)	119·6(2)
		C(N8)—C(P'1)—C(P'6)	121·9(2)
		C(P'2)—C(P'1)—C(P'6)	118·5(2)
		C(P'1)—C(P'2)—C(P'3)	120·3(2)
		C(P'2)—C(P'3)—C(P'4)	120·7(2)
		C(P'3)—C(P'4)—C(P'5)	119·3(2)
		C(P'4)—C(P'5)—C(P'6)	121·0(2)
		C(P'1)—C(P'6)—C(P'5)	120·2(2)

**7**

the facing phenyl rings in **2** and **3** have been attributed to steric repulsion, which also causes a considerable distortion of the σ -framework of the basal naphthalene moiety.^{3,4} On the other hand, the short distance between the facing pyrene rings in **7**, which is comparable to those in **5** and **6**, has been interpreted as due to the attractive force resulting from the 'excimer-like'

π - π interaction.¹⁵ The rotation angles (θ) for both of the aromatic rings with reference to the basal naphthalene plane are similar (59–62°) in the cations **5** and **6**. Further, the values of the dihedral angle (φ) between two single bonds connecting the substituents are also similar in **5** and **6** suggesting that the basal naphthalene moieties in **5** and **6** suffer from a similar σ -framework distortion.

In order to make a comparison with the x-ray crystallographic data, we carried out AM1 calculations (using the AMPAC system; QCPE 527)¹⁶ on cations **5** and **6**, with the rotation angles (θ) of both of the substituents varied by 10° with respect to the naphthalene plane. The calculated heat of formation was plotted against the rotation angle to give the results shown in Figures 8 and 9. In both of the cations, the structures with the aromatic rings taking the conformation perpendicular to the basal naphthalene are calculated to be the local maxima in energy due to loss of π -conjugation; this

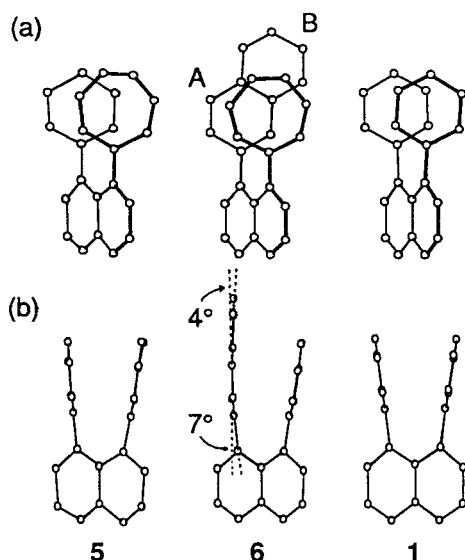


Figure 7. (a) Head-on views and (b) side views of the structures of **5**, **6** and **1** determined by x-ray crystallography. Hydrogen atoms are omitted for clarity

structure is calculated to be $1.2 \text{ kcal/mol}^{-1}$ ($1 \text{ kcal} = 4.184 \text{ kJ}$) less stable than the optimized structure for the case of cation **5**. The energy minimum is located at a rotation angle range $\theta = 40\text{--}50^\circ$ for **5**. This value is $10\text{--}20^\circ$ smaller than the experimental value of 61° (Table 5), although the energy difference is only about $0.1 \text{ kcal/mol}^{-1}$. Although small in energy difference, the AM1 calculations apparently tend to take account of the π -conjugation more significantly than was observed experimentally. For the cation **6**, two energy minima are found at $\theta \approx 50^\circ$ and 140° with a ring flipping barrier of *ca* $1.1 \text{ kcal/mol}^{-1}$. The experimentally determined structure has $\theta = 59^\circ$ for the tropylium ring and 62° for the 2-naphthyl group, and is fairly close to the calculated structure with $\theta = 50^\circ$, which is slightly more stable than that with $\theta = 140^\circ$. The top views of the fully minimized structures calculated by AM1 for **5** and **6** are shown in Figure 10 together with those obtained by x-ray crystallography. It should be noted that the neutral aromatic rings are more attracted toward the tropylium face than was expected from calculations.

The x-ray structures shown in Figures 7 and 10 indicate that the van der Waals repulsion between the

Table 5. Structural characteristics of 1,8-diarylnaphthalenes

Compound	Some short distances (Å)							Angles (°)		
	<i>peri</i> ^a	A—A'	A—B'	A—C'	B—B'	B—C'	C—C'	Splay, ϕ ^b	Rotation, θ ^c	Single bonds, φ ^d
5	2.53	3.23	2.94	3.19	3.00	2.93	3.25	16	61 (Ph) 61 (T)	10
6	2.549	3.145	2.952	3.235	2.941	2.884	3.232	13 ^e 9 ^f	62 (N) 59 (T)	11.4
1 ^g	2.566 (2.563)	3.283 (3.289)	3.048 (3.052)	3.332 (3.338)	2.996 (2.993)	3.031 (3.031)	3.294 (3.304)	20 (20)	67 (67)	3.4 (3.4)
2 ^h	2.600	3.431	3.041	3.258	3.107	3.039	3.427	25	57	10.0
3 ⁱ	2.510	3.376	3.137	3.758	2.945	3.127	3.372	37	58	33.3
7 ^j	2.571	3.229	2.964	3.179	2.997	2.922	3.256	15	58	10.2

^a Distance between *peri*-carbons of the basal naphthalene.

^b Splayed-out angle of the facing aryl rings.

^c Rotation angle of the substituent rings against the basal naphthalene plane. Ph = phenyl; N = naphthyl; T = tropylium.

^d Dihedral angle between two single bonds which connect aromatic rings.

^e Splayed-out angle between the best planes of tropylium ring and A-ring of the 2-naphthyl group.

^f Splayed-out angle between the best planes of tropylium ring and B-ring of the 2-naphthyl group.

^g Data from Ref. 2b in parentheses.

^h Data from Ref. 3.

ⁱ Data from Ref. 4.

^j Data from Ref. 16.

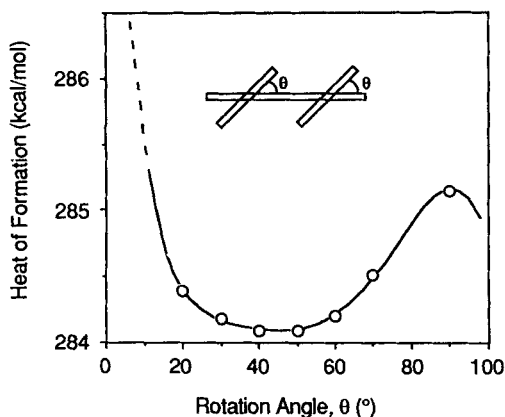


Figure 8. Plot of the heat of formation of the cation **5** calculated by AM1 versus the rotation angle, θ

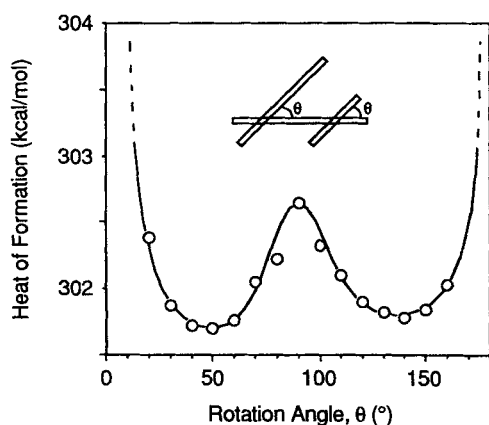


Figure 9. Plot of the heat of formation of the cation **6** calculated by AM1 versus the rotation angle, θ

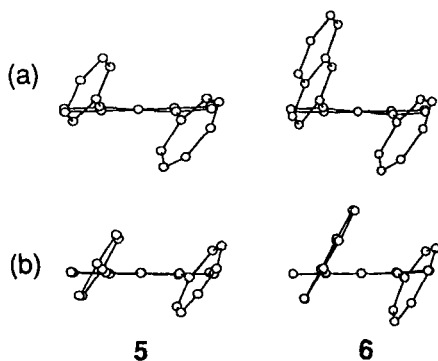


Figure 10. Top views for the structures of the cations **5** and **6**: (a) calculated by AM1; (b) determined by x-ray crystallography. Hydrogen atoms are omitted for clarity

facing rings is considerably diminished by the attractive force counteracting between them. This attractive force can probably be ascribed to the intramolecular charge-transfer interaction, which can be detected by electronic spectroscopy⁵ and was shown to enhance the intrinsic thermodynamic stability of the tropylium-ion acceptor.⁵ Thus, in conclusion, the results of the x-ray structure analysis provided clear evidence that the intramolecular charge-transfer interaction significantly affects the molecular structure to an extent that almost offsets the effect of van der Waals interaction.

SUPPLEMENTARY MATERIAL

Tables of atomic coordinates and thermal parameters for **5**·SbF₆⁻, **6**·SbF₆⁻ and **1** are available from the authors on request.

REFERENCES

- W. L. Jorgensen and D. L. Severance, *J. Am. Chem. Soc.* **112**, 4768–4774 (1990); (b) C. A. Hunter and J. K. M. Sanders, *J. Am. Chem. Soc.* **112**, 5525–5534 (1990), (c) F. Cozzi, M. Cinquini, R. Annunziata, T. Dwyer and J. S. Siegel, *J. Am. Chem. Soc.* **114**, 5729–5733 (1992), and references cited therein.
- (a) H. O. House, R. W. Magin and H. W. Thompson, *J. Org. Chem.* **28**, 2403–2406 (1963); (b) R. A. Ogilvie, PhD Thesis, Massachusetts Institute of Technology (1971); (c) R. L. Clough, P. Mison and J. D. Roberts, *J. Org. Chem.* **41**, 2252–2255 (1976).
- R. L. Clough, W. J. Kung, R. E. Marsh and J. D. Roberts, *J. Org. Chem.* **41**, 3603–3609 (1976).
- P. G. Evrard, P. Piret and M. V. Meerssche, *Acta Crystallogr., Sect. B* **28**, 497–506 (1972).
- (a) K. Komatsu, N. Abe, K. Takahashi and K. Okamoto, *J. Org. Chem.* **44**, 2712–2717 (1979); (b) R. Tsuji, K. Komatsu, Y. Inoue and K. Takeuchi, *J. Org. Chem.* **57**, 636–641 (1992).
- Crystallographic Data Centre, Cambridge, UK; only the crystal data but no data for atomic coordinates are available for **1**.
- G. M. Sheldrick, in *Crystallographic Computing 3*, edited by G. M. Sheldrick, C. Kruger, and R. Goddard, pp. 175–189. Oxford University Press, Oxford (1985).
- TEXSAN, *Crystal Structure Analysis Package*. Molecular Structure Corp., Woodlands, TX (1985 and 1992).
- N. Walker and D. Stuart, *Acta Crystallogr., Sect. A* **39**, 158–166 (1983).
- P. T. Beurskens, G. Admiraal, G. Beurskens, W. P. Bosman, S. Garcia-Granda, R. O. Gould, J. M. M. Smits and C. Smykalla, *DIRDIF92, The DIRDIF Program System, Technical Report of the Crystallography Laboratory*, University of Nijmegen, Nijmegen (1992).
- D. T. Cromer and J. T. Waber, in *International Tables for X-ray Crystallography*, Vol. IV, Table 2.2A. Kynoch Press, Birmingham (1974).
- J. A. Ibers and W. C. Hamilton, *Acta Crystallogr.* **17**, 781–782 (1964).

13. D. C. Creagh and W. J. McCauley, in *International Tables for Crystallography*, edited by A. J. C. Wilson, Vol. C, Table 4.2.6.8, pp. 219–222. Kluwer, Boston (1992).
14. D. C. Creagh and J. H. Hubble, in *International Tables for Crystallography*, edited by A. J. C. Wilson, Vol. C, Table 4.2.4.3, pp. 200–206. Kluwer, Boston (1992).
15. P. Wahl, C. Krieger, D. Schweitzer and H. A. Staab, *Chem. Ber.* **117**, 260–276 (1984).
16. M. J. S. Dewar, E. G. Zoebisch, E. F. Healy and J. J. P. Stewart, *J. Am. Chem. Soc.* **107**, 3902–3909 (1985).